



Review

Methane Emission Reduction Technologies for Natural Gas Engines: A Review

Andrew Huonder * and Daniel Olsen

Department of Mechanical Engineering, Colorado State University, Fort Collins, CO 80523, USA; daniel.olsen@colostate.edu

* Correspondence: andrew.huonder@colostate.edu

Abstract: This review summarizes technologies to reduce methane emissions from natural gas engines with a focus on exhaust treatment. As regulations on methane emissions from natural gas facilities become more restrictive, methane emission reduction technologies become increasingly important. Methane is the second most prevalent human-generated greenhouse gas. In 2020, 197,000 metric tons of methane were released as a result of methane slip. In-cylinder methods such as optimized valve timing and crevice volume reduction are effective in reducing methane slip. Exhaust treatment methods such as catalytic oxidizers and regenerative thermal oxidizers can achieve near 100% methane reduction under certain conditions. Implementation of hydrogen blending and exhaust gas recirculation systems results in a decrease in methane emissions of between 20 and 30%. Future research should focus on testing full-scale catalytic oxidation systems on lean-burn natural gas engines. Research should also focus on implementing regenerative thermal oxidizers on natural gas engines, as well as combining hydrogen blending with these techniques.

Keywords: methane emissions; natural gas engines; catalytic oxidation; regenerative thermal oxidation; hydrogen blending



Citation: Huonder, A.; Olsen, D. Methane Emission Reduction Technologies for Natural Gas Engines: A Review. *Energies* **2023**, *16*, 7054. https://doi.org/10.3390/en16207054

Academic Editor: Constantine D. Rakopoulos

Received: 23 August 2023 Revised: 30 September 2023 Accepted: 8 October 2023 Published: 12 October 2023



Copyright: © 2023 by the authors. Licensee MDPI, Basel, Switzerland. This article is an open access article distributed under the terms and conditions of the Creative Commons Attribution (CC BY) license (https://creativecommons.org/licenses/by/4.0/).

1. Introduction

Methane (CH₄) is the second most abundant human-generated greenhouse gas behind carbon dioxide (CO₂). In 2021, 12% of human-generated greenhouse gas (GHG) emissions were methane [1]. There were 25,980,000 metric tons of methane emitted in 2021 [2]. Although methane has a significantly shorter lifespan in the atmosphere than CO₂, methane is 25 times more effective at trapping heat in the atmosphere [3,4]. The concentration of methane in the atmosphere has doubled within the last 200 years and, currently, 20% of all global emissions (human-created and natural) is methane [3]. As the world focuses on the reduction in greenhouse gas emissions, the implementation of hydrogen fuel has become a prevalent research topic. The burning of hydrogen produces no carbon emissions, making it a relatively clean fuel to burn [5–10].

Figure 1 shows EPA-reported data for sources of methane emissions in the United States. Natural gas is primarily composed of methane, between 70 and 90% [11]. Methane emissions from natural gas and petroleum sources are the leading source of methane emissions [1]. One of the main uses for natural gas is power generation. Approximately 38% of the United States' natural gas consumption in 2022 was for electrical power generation [12]. According to the Energy Information Administration (EIA), in 2022, there were roughly 1500 operable natural gas internal combustion engines in the United States being used for power generation [13]. The United States' natural gas consumption for transportation was 5% in 2022. This includes natural gas engines that are used to drive compressors on gas pipelines, as well as natural gas engines that are used in vehicles [12]. The EIA reports that there are more than 1400 interstate natural gas compression stations that use natural gas engines in the United States [14]. Compressor stations on smaller, intrastate pipelines

Energies 2023, 16, 7054 2 of 18

that move natural gas from wells to the interstate pipelines are larger in number and use primarily natural gas internal combustion engines for compression.

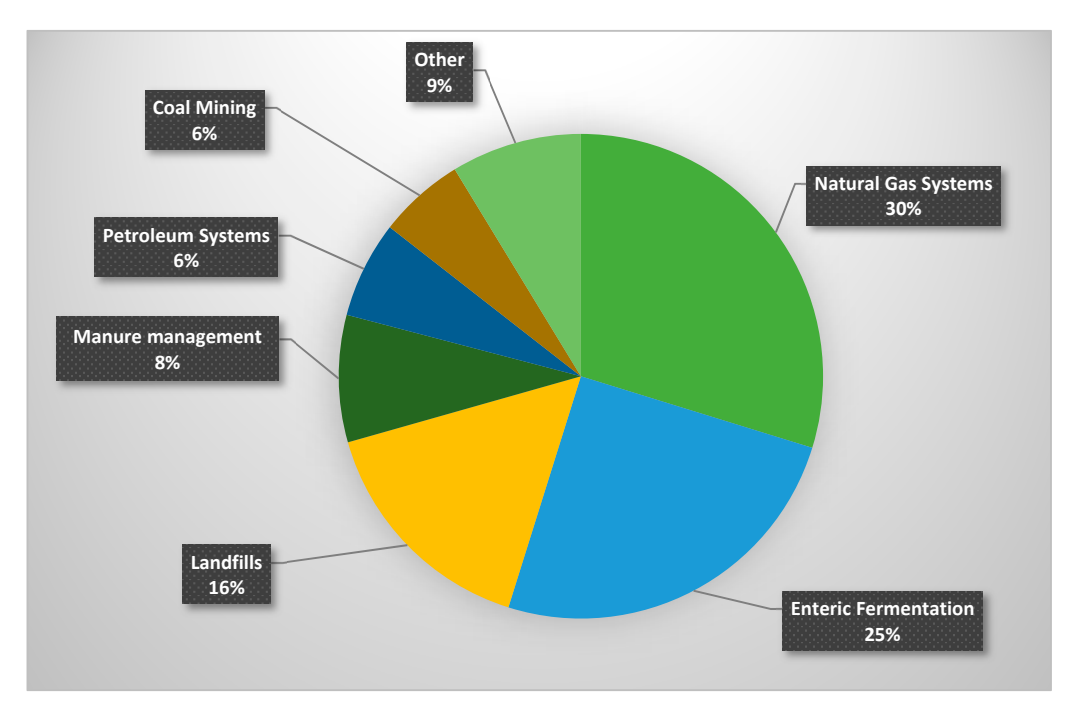


Figure 1. EPA-reported estimates of sources of methane using data from 1990–2021 [2].

Methane slip is a term that refers to methane that does not combust in a combustion engine. Methane emissions due to methane slip in natural gas systems were 197,000 metric tons in 2020 [2]. Methane slip resulted in 3.0% of all methane emissions from natural gas systems in 2020 [2]. Lean-burn natural gas engines result in higher methane emissions than stoichiometric natural gas engines. Stoichiometric engines, also known as "rich-burn" natural gas engines, are engines that operate at approximately stoichiometric, though slightly rich, air-fuel ratios. Stoichiometric engines result in more complete combustion and less unconsumed methane being released via the exhaust than lean-burn natural gas engines [15]. In a study, a 4-stroke stoichiometric engine produced 0.23 lb. of CH₄ per MMBtu while a 4-stroke lean-burn engine produced 1.25 lb. of CH₄ per MMBtu [16]. Stoichiometric engines typically use three-way catalysts that are effective at reducing methane emissions and are partly responsible for lower methane emissions from this engine class. However, three-way catalysts are designed for stoichiometric engines and are not effective for lean-burn natural gas engines [15]. Lean-burn natural gas engines are more efficient and are commonly chosen over stoichiometric engines where minimizing fuel consumption is favored. By finding effective methane emission reduction methods for lean-burn natural gas engines, the amount of methane released into the atmosphere can be reduced.

The greenhouse gas reporting program (GHGRP), which was codified by Title 40 (Protection of Environment) of the code of federal regulations, is used to monitor sources of greenhouse gas emissions around the country. Facilities are required to report their greenhouse gas emissions under the GHGRP [17]. Subpart W of the GHGRP requires petroleum and natural gas facilities that emit the equivalent of 25,000 metric tons of CO₂ of greenhouse gases a year to report their emissions data to the Environmental Protection Agency (EPA) [18]. Under the Inflation Reduction Act, starting in 2024, facilities that are required to report to the EPA under subpart W will be required to pay \$900 per metric ton of CH₄ emitted. This monetary value will increase to \$1200 in 2025 and to \$1500 in 2026 and beyond [19]. For reference, if a facility emits 900 metric tons of CH₄, the equivalent of 25,000 metric tons of CO₂, in 2026, it will be charged \$1.5 million dollars. The EPA-

Energies **2023**, 16, 7054 3 of 18

proposed "Good Neighbor Plan" will require upwind states to decrease their greenhouse gas emissions, including methane, to benefit downwind states [20]. Under subpart JJJJ in the new source performance standard (NSPS), the emissions of stationary natural gas engines are regulated by their emission of volatile organic compounds (VOC). Non-emergency natural gas more powerful than 100 HP is restricted to either 0.7 g/HP-h or 80 ppmvd (parts per million by volume, dry) at 15% O_2 [21]. VOCs are defined as non-methane and nonethane hydrocarbons, so they do not include methane [22]. Aldehydes are also excluded from the VOCs. Methane emissions are targeted in impending regulations through the Inflation Reduction Act and Good Neighbor Plan [19,20]. Once these are implemented, the need for technologies to decrease methane emissions becomes more important.

2. Sources of Methane Slip in Natural Gas Engines

Methane slip refers to methane that does not combust in the operation of a natural gas engine. Between 1% and 5% of the total methane can "slip" through the system [23]. There are several sources of methane slip in the operation of a natural gas engine, including blow-by, valve overlap, and incomplete combustion.

In a numerical analysis of a lean-burn 4-stroke dual-fuel engine, valve overlap resulted in around 30% of the total methane slip at full load [24]. Incomplete combustion from crevices and quenching contributed to the other 70%. Blowby was not considered in this analysis. In this study, valve overlap and incomplete combustion from crevices each resulted in the emission of around 10 g of CH_4 per kWh at any load. Methane slip due to quenching caused 10 g of CH_4 per kWh at full load, and 55 g of CH_4 per kWh at 25% load.

Blow-by, shown in Figure 2, is when methane leaks between the piston ring and the cylinder wall into the crankcase. Unlike the other sources of methane slip, blow-by does not result in unburned methane in the exhaust and therefore is not able to be treated by any exhaust treatment. Blow-by can result in up to 25% of the methane emissions from a natural gas engine [25].

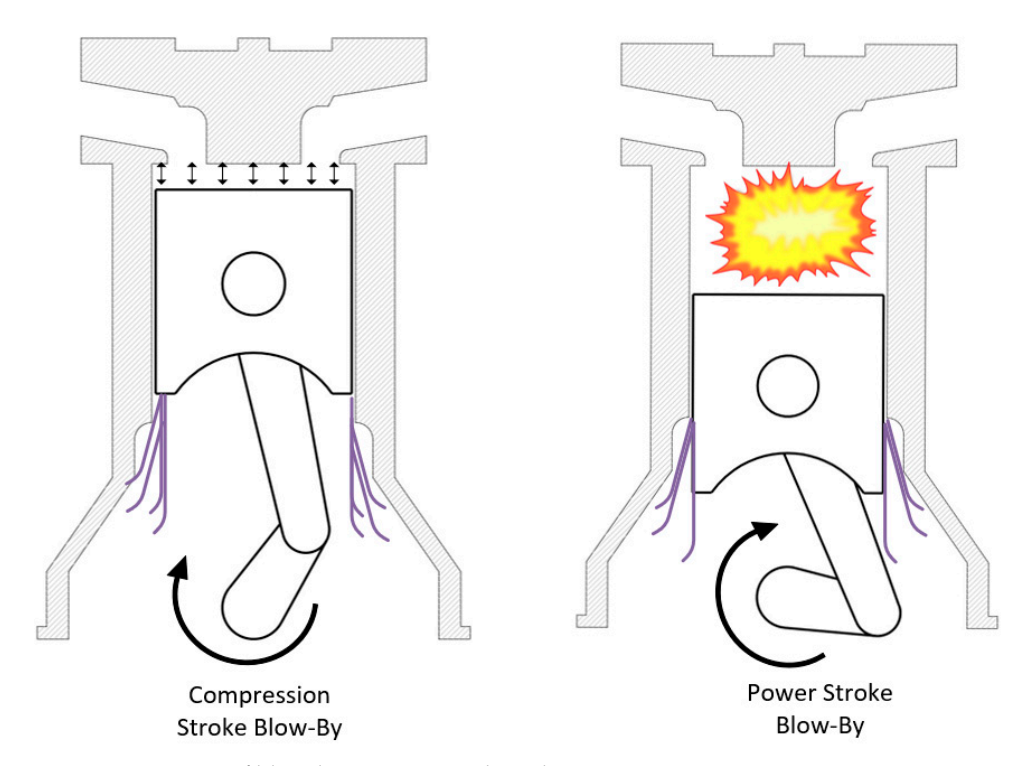


Figure 2. Diagram of blow-by in an internal combustion engine.

Valve overlap, as seen in Figure 3, occurs when both the inlet and outlet valves are open, and methane bypasses the combustion process and passes into the exhaust. Valve overlap occurs at the end of the exhaust stroke and the beginning of the intake stroke.

Energies **2023**, 16, 7054 4 of 18

During the exhaust stroke (upstroke), the exhaust is forced out of the cylinder through the exhaust valve. The inlet valve opens as the piston approaches the top dead center. There is a period when both the inlet and exhaust valves are open at the same time. During this time, the high pressure of the incoming gas flows to the low pressure of the exhaust, causing methane to go directly from the inlet manifold to the exhaust manifold, resulting in unburned fuel in the exhaust [23].

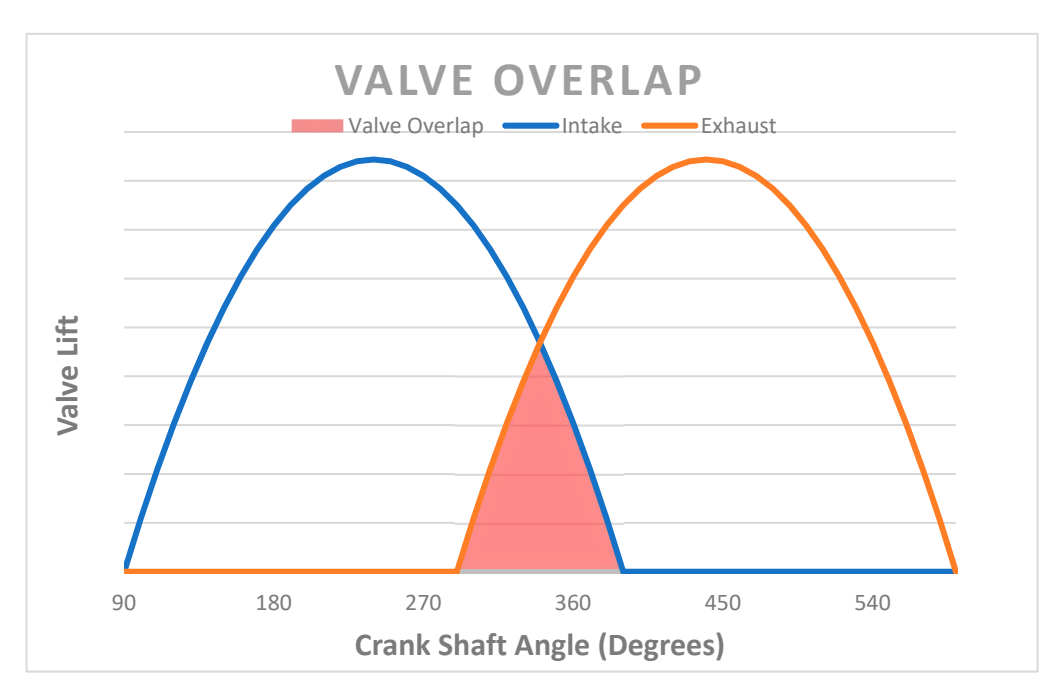


Figure 3. Diagram of valve overlap occurring between exhaust and intake stroke.

Incomplete combustion can be a result of trapped methane in crevices, quenching near walls, and quenching in lean mixture zones. Crevices (high surface/volume ratio regions) can restrict flame propagation into these volumes allowing methane to go unburned [15]. The amount of unburned hydrocarbons increases exponentially with crevice volume [26]. Quenching effects can also result in incomplete combustion. A quenching effect can occur near the walls of the cylinder. Heat is lost from the gas to the cylinder wall, decreasing the temperature of the gas, and not allowing combustion to occur. Quenching can also occur when there are areas of high λ . Lambda (λ) is the ratio of the actual air–fuel ratio to the stoichiometric air–fuel ratio. In areas of high λ , there is not enough fuel for combustion to occur.

3. In Cylinder Methane Emission Reduction Technologies

One way to decrease blow-by is to decrease the clearance between the piston ring and the cylinder wall, improving the seal and decreasing the amount of gas that can slip into the crankcase, and decreasing the crevice volume where fuel can be protected from the flame. The tradeoff is the improved seal increases the frictional resistance of the piston, decreasing the efficiency of the engine. The methane that leaks into the crankcase creates pressure in the crankcase that needs to be vented. The vented methane from the crankcase can be recycled back into the engine but needs to be filtered. Any oil in the methane that was picked up in the crankcase needs to be removed or damage to the engine may occur [23]. The crevice volume can also be reduced by decreasing the distance between the top ring and the top of the piston. However, this may result in diminished piston reliability since the top ring would be closer to high temperature combustion gases.

Methane slip from valve overlap can be reduced by optimizing the timing for the valves. Valve overlap is necessary because it maximizes the fuel–air mixture mass in the

Energies 2023, 16, 7054 5 of 18

cylinder, maximizing performance [23]. Due to the benefits, valve overlap is tolerable considering it only results in minimal methane slip.

One way to decrease quenching effects in the combustion chamber is to operate the engine closer to stoichiometric [15]. With more fuel (or less air) in the combustion chamber, there is a reduced chance of higher λ areas or heat loss to the cylinder walls resulting in quenching. When operating with a richer mixture, more nitrogen oxides (NO_x) are created due to the higher combustion temperatures [27]. For a lean-burn natural gas engine, running richer is typically not an option due to NO_x permit limits. Controlled auto-ignition is a method that results in stable combustion and less unburned fuel, which has been demonstrated in a 4-stroke industrial natural gas engine [28]. Having improved air-fuel mixing to create a homogenous mixture can reduce high λ areas and decrease quenching in a lean-burn natural gas engine [15]. High-pressure fuel injection is one approach for improving mixing on large bore natural gas integral compressor engines [29]. High pressure fuel injection and precombustion chamber ignition can reduce the frequency of partial combustion and misfires leading to fewer methane emissions [30]. Directional pre-combustion chambers can be designed to target zones of unburned methane to promote more complete oxidation. This approach is demonstrated through CFD simulations in a large bore natural gas 2-stroke engine through design changes to the pre-combustion chamber nozzle [31]

4. Exhaust Methane Emission Reduction Technologies

4.1. Catalytic Oxidation

Catalytic oxidation is a process in which the exhaust flows over a catalyst, usually a precious metal like palladium or platinum in the case of a methane oxidizer. The precious metals are typically dispersed in a porous washcoat such as alumina or ceria that is supported by a metal or ceramic substrate. The catalyst lowers the chemical activation energy thereby accelerating the process of methane reacting with oxygen to produce CO₂ and H₂O. Catalytic oxidizers can be susceptible to poisoning and aging. Catalytic poisoning is a deactivation of the catalyst. This can be a result of the poison chemically altering the catalyst causing it to be less effective or it could simply physically block the catalyst from reacting with the methane [32]. Hydrogen Sulfide (H₂S) can be present in natural gas at concentrations as high as 5% [11]. The presence of hydrogen sulfide in the combustion process results in sulfur dioxide (SO₂) being produced and present in the exhaust of natural gas engines [33]. A concentration as low as 20 ppm of SO₂ can be detrimental to a catalyst's performance [34]. The source of sulfur in a natural gas engine's exhaust can be from the natural gas itself but it can also be from the lubrication oil of the engine [33].

Figure 4 plots methane conversion vs. temperature for catalyst studies reported in the literature. The yellow symbol represents the palladium catalyst, purple represents the platinum catalyst, red represents the platinum–palladium alloy catalyst, orange represents the rhodium catalyst, and blue represents the nickel-magnesium alloy. Each catalyst has an ellipsoid to group the catalyst's performance range. The shaded sections represent exhaust temperature ranges for 4-stroke and 2-stroke lean-burn natural gas engines. The exhaust temperature range for 2-stroke lean-burn natural gas engines is 280–380 °C. For 4-stroke lean-burn natural gas engines, it is 395–520 °C [29,35,36]. Light gray represents 2-stroke and dark gray represents 4-stroke.

Platinum and nickel-magnesium catalysts are unable to achieve 100% methane conversion at low enough temperatures for either type of lean-burn natural gas engine. Palladium and rhodium catalysts could achieve 100% conversion at temperatures within the 4-stroke temperature range but not the 2-stroke temperature range. The platinum-palladium catalyst is the only catalyst that could achieve 100% conversion within the temperature range of the 2-stroke natural gas engine. The overwhelming majority of studies focusing on the oxidation of methane, including the ones summarized in Figure 4, are small-scale tests either using bottled gas or just a portion (i.e., slipstream) of the exhaust of a natural gas engine. There were no full-scale methane oxidation catalyst engine studies found in the

Energies 2023, 16, 7054 6 of 18

literature. Furthermore, the methane oxidation catalysts studied are under development and are not commercially available.

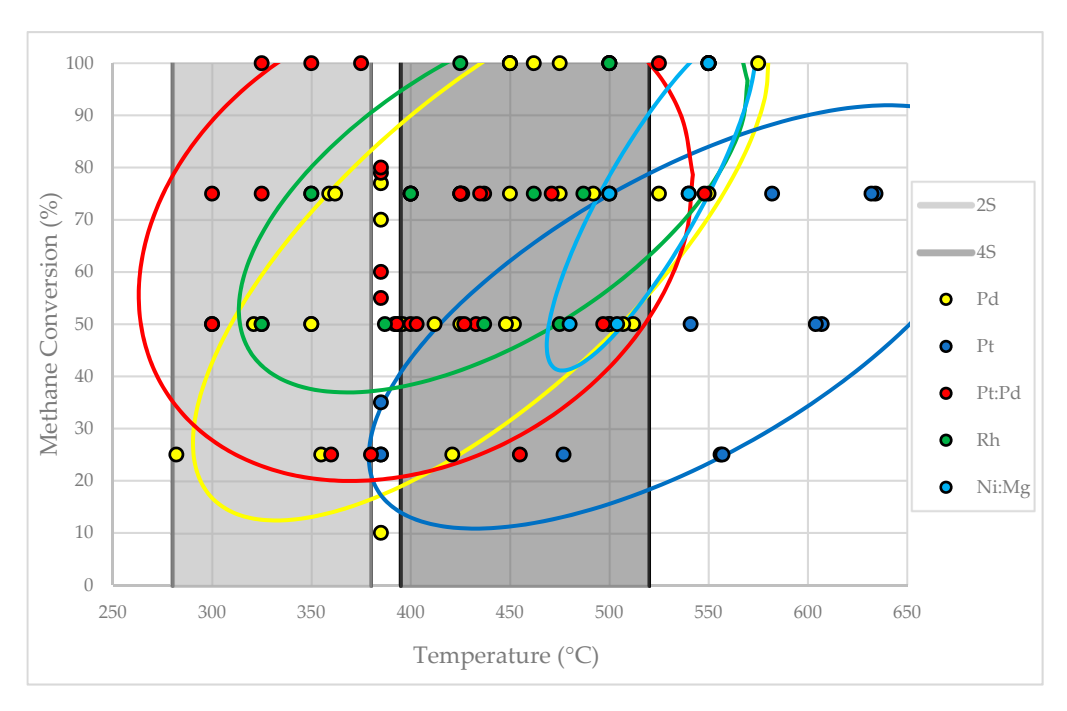


Figure 4. Percentage of methane conversion for Pd, Pt, Pt:Pd, Rh, and Ni:Mg catalysts with respect to gas temperature, data from [34,37–41], including exhaust temperature ranges for 2-stroke and 4-stroke lean-burn natural gas engines, data from [29,35,36]; data used to generate this figure are summarized in Table A1.

4.1.1. Palladium

Palladium is a common precious metal selected as a methane oxidation catalyst and has been studied heavily [34,37–78]. Palladium is capable of 100% methane conversion at temperatures as low as 450 °C [40]. Palladium is effective in methane oxidation at the exhaust temperatures for a 4-stroke lean-burn natural gas engine, but its threshold is not low enough to be fully effective for a 2-stroke natural gas engine [29,35,36]. The most difficult challenge with palladium as a methane oxidation catalyst is its susceptibility to aging and poisoning. At a constant temperature of 385 °C, a palladium catalyst dropped from 70% to 10% methane conversion after 1500 h of use [37]. When a palladium catalyst was hydrothermally aged, the T_{75} (temperature to achieve 75% methane conversion) increased from 359 °C to 492 °C, a 21% increase [39]. When SO_2 is present in the methane stream, the palladium becomes poisoned. With the presence of 20% SO_2 , the T_{100} value increased by 12% [34].

4.1.2. Platinum

Platinum is another common choice for a methane oxidation catalyst. There are many studies on platinum catalysts for methane [37,39,40,42,50,53,62,67,69,74,79–82]. The required temperature for a solely platinum catalyst is much higher than the operating range of both 4-stroke and 2-stroke engines [29,35,36]. The benefit of a platinum catalyst is that it is less susceptible to the effects of aging and poisoning than a catalyst like palladium. As noted above, palladium had an increase in T_{75} of 359 °C to 492 °C, a 21% increase, after hydrothermal aging. After the same hydrothermal aging process platinum had only a 6% increase in temperature going from 541 °C to 632 °C [39]. At a constant temperature of 385 °C, a platinum catalyst dropped from 35% to 25% methane conversion after 1500 hours of use, significantly better than the performance of palladium [37].

Energies 2023, 16, 7054 7 of 18

4.1.3. Palladium-Platinum Alloy

To have the high aging and poisoning resistivity of platinum and the lower temperature requirement of palladium, the two metals are often combined into an alloy [37–39,48–51,53,62,67,69,74,81–84]. The ratios of platinum to palladium range from 1:5 to 5:1 [37–40]. The Pt-Pd alloy results in a wide range of performances based on this ratio. A T_{100} value as low as 325 °C and as high as 525 °C is achieved. After 1500 hours of use, the methane conversion rate for a Pt-Pd alloy (1:1) dropped from 79% to 60%, while the conversion rate for a Pt-Pd alloy (2:3) dropped from 80% to 55% at 385 °C [37]. For a Pt-Pd alloy (4:1), the T_{75} value increased by 14% after hydrothermal aging, compared to the palladium and platinum catalysts, which had increases of 21% and 6%, respectively [39]. While not as resistant to aging as the platinum catalyst, Pt-Pd catalysts achieve methane oxidation at lower temperatures. The T_{75} of the Pt-Pd alloy without aging was 437 °C, significantly lower than the T_{75} value for the platinum catalyst, which was 582 °C [39].

4.1.4. Rhodium

Rhodium catalysts are effective in 4-stroke lean-burn natural gas engines but require temperatures too high to operate effectively in 2-stroke engines. Rhodium is an understudied catalyst for methane oxidation [34,74,77]. Palladium catalysts are relatively resistant to sulfur poisoning while in dry conditions; however, they are much more susceptible to sulfur poisoning while in wet conditions [34]. A variety of rhodium-based catalysts were tested and compared to a palladium catalyst with the presence of water and sulfur. The catalysts used were a 2% by-weight palladium catalyst using a ZSM-5 (SiO₂/Al₂O₃) washcoat and a 2% by-weight Rhodium Catalyst also using a ZSM-5 washcoat. Under standard conditions with no H₂O or SO₂ present, the rhodium catalyst achieved 100% methane conversion at a temperature of 425 °C and the palladium achieved it at a temperature of 462 °C. When H₂O and SO₂ were introduced into the fuel stream, the T₁₀₀ values for rhodium increased to 550 °C. The palladium catalyst was not able to achieve 100% conversion and only achieved 95% at the peak temperature of 600 °C. For reference, the rhodium achieved 95% at 500 °C [34]. The main drawback of using rhodium is that it is much more expensive than palladium and platinum. In the last 10 years, the cost of palladium has been about \$60/g and platinum has been approximately \$35/g. In that same time frame, rhodium has reached as high as \$900/g and is usually well over \$100/g [85].

4.1.5. Nickel-Magnesium Alloy

A catalyst consisting of a nickel magnesium alloy has been used as an alternative to palladium, which is susceptible to being degraded with a high concentration of water [41,86–92]. After 40 hours of use, a pallidum catalyst's T_{100} value increased from 450 °C to 575 °C when used with a methane stream including 10% H_2O . By comparison, in the same conditions, the T_{100} value for a Ni-Mg (9:1) catalyst remains constant at 550 °C after 40 hours [41]. However, 550 °C is higher than the exhaust temperature range for both 4-stroke and 2-stroke lean-burn natural gas engines. More work would have to be done to determine if a nickel-magnesium catalyst can be effective for natural gas lean-burn engines.

4.1.6. Three-Way Catalyst

A three-way catalyst is used to reduce nitrogen oxides (NO_x) and oxidize; carbon monoxide (CO); and hydrocarbons (HC), including methane [93,94]. Three-way catalysts are effective at reducing the emissions of all three and can ideally achieve a near 100% emission reduction [94]. A study performed on a stoichiometric 4-stroke natural gas engine using a three-way catalyst reported catalytic destruction of methane from 1.4 g/bhp-h to 0.6 g/bhp-h, a 57% reduction. For the same datapoint the result showed a 100% reduction in NO_x , from 11.4 g/bhp-h to 0 g/bhp-h, and a 98% reduction in CO emissions, from 8.75 g/bhp-h to 0.2 g/bhp-h [95]. Three-way catalysts are made of many of the same metals that can be used for lean-burn natural gas engine oxidation catalysts such as platinum, palladium, and rhodium. However, three-way catalysts are specifically tuned to reduce the

Energies 2023, 16, 7054 8 of 18

emissions of NO_x , CO, and HC at stoichiometric conditions ($\lambda \approx 1$) [15,93]. A three-way catalyst uses NO_x as an oxidizer. As the λ value increases and the concentration of NO_x in the exhaust decreases. The three-way catalyst becomes less effective at oxidizing HC and reducing NO_x emissions. As λ increases, CO oxidation efficiency is relatively unaffected. In a study, at $\lambda = 1$, NO_x reduction efficiency and HC oxidation efficiency was near 100%. At $\lambda = 1.1$, the NO_x reduction efficiency dropped to 10% and the HC oxidation efficiency dropped to 55% [93]. For stoichiometric natural gas engines, a three-way catalyst is quite effective, but to have effective methane reduction for lean-burn natural gas engines, a catalyst other than a three-way catalyst needs to be used.

4.2. Thermal Oxidizers

One method to oxidize methane that does not require a catalyst is a regenerative thermal oxidizer (RTO). Many RTOs consist of two porous heat beds connected by an oxidation chamber [96]. Figures 5 and 6 show schematics of two different RTOs. The heat beds are usually made from ceramic but there are instances where they are made of gravel supported by a steel structure [96,97]. In an RTO, the exhaust gas containing methane flows through the first heat bed, which acts as a preheater. Once the exhaust reaches the target temperature, the methane oxidizes and releases heat. Methane oxidation releases 802.7 kJ/mol, as seen in eqn. 1 [98]. The gas then leaves the oxidation chamber and transfers heat to the second heat bed, which acts as a heat sink. To maintain this process, flow through the RTO is periodically reversed, and the second bed becomes the preheater and the first bed becomes the heat sink. The system eventually reaches steady state and is self-sustaining. The energy released from the oxidation process provides heat to sustain the process. When an RTO is initially started, energy is required to heat the gas to instigate oxidation. Electrical heaters are used in the oxidation chamber to achieve this. These heaters can be in the range of 22–40 kW depending on the size of the RTO [96–99].

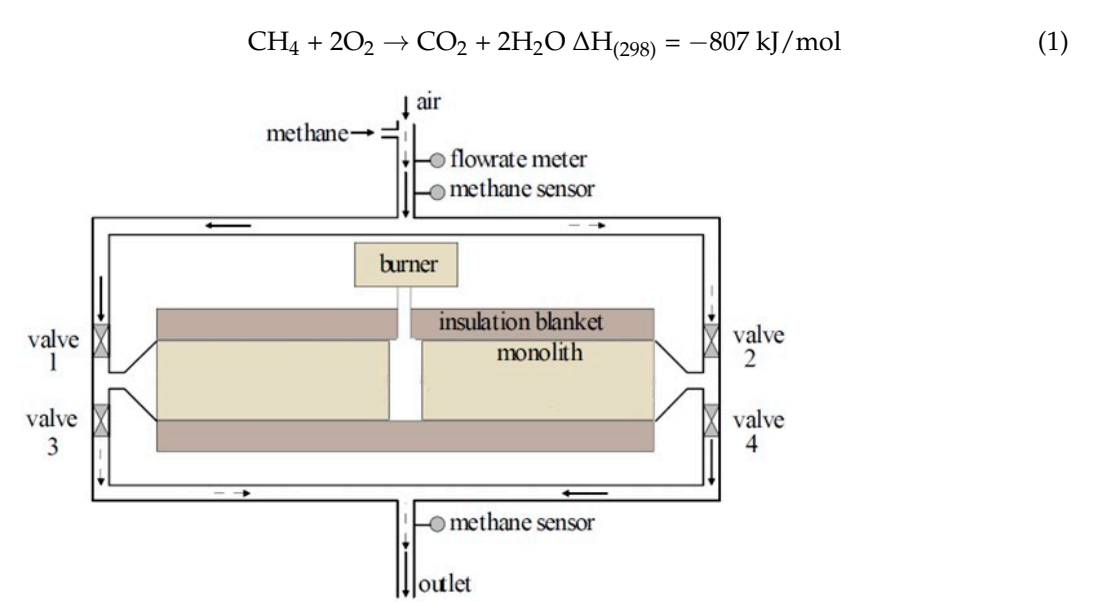


Figure 5. RTO schematic in which valves 1 and 4 open for flow to go left to right and valves 2 and 3 for flow to go right to left Adapted with permission from Ref. [99].

The primary use of RTOs has been to oxidize methane gas from ventilation air methane (VAM) from coal mines [100]. Due to their size and complexity, there have not been many applications for using RTOs on natural gas engines. The benefit of using an RTO to oxidize methane in the exhaust of a lean-burn natural gas engine is that no matter the temperature of the exhaust gas, it can be heated to induce oxidation. The exhaust temperature range for 2-stroke and 4-stroke lean-burn natural gas engines are 280–380 °C and 395–520 °C, respectively [29,35,36]. There may not be a need for heat to be added for a 4-stroke engine

Energies **2023**, 16, 7054 9 of 18

operating within the higher range of exhaust temperatures. For the lower end of the exhaust temperature range for 4-stroke and for the entire 2-stroke exhaust temperature range, heat will need to be added to the combustion chamber to induce oxidation. Table 1 summarizes results from RTO performance studies reported in the literature [90–92,96].

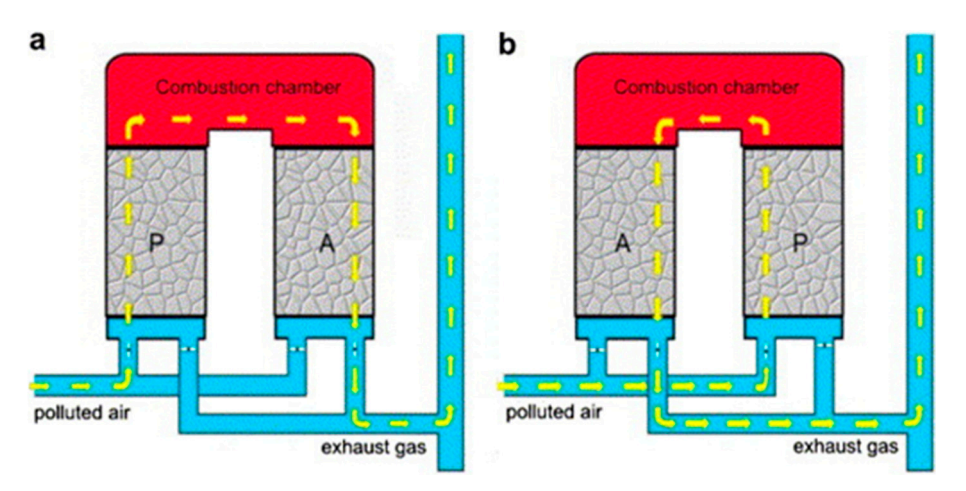


Figure 6. RTO schematic in which flow switches from clockwise (**a**) to counterclockwise (**b**). Adapted with permission from Ref. [96].

Regenerative Catalytic Oxidizers (RCO) have a similar layout to an RTO but have a catalyst in the heat bed. This can decrease the operating temperature required for complete oxidation, with many RCOs requiring 320–430 $^{\circ}$ C while RTOs require ranges closer to 760–820 $^{\circ}$ C. A study using an RCO on natural gas/diesel dual-fuel engines saw a more than 90% reduction in hydrocarbon emissions [101]. This RCO operated at temperatures between 300 and 700 $^{\circ}$ C.

Operational	Heated Wire	Methane	Methane Removal	Source
Temperature	Power	Concentration	Efficiency	
300-513 °C	40 kW	1190 ppm	91.5%	[97]
300-382 °C	40 kW	21 ppm	95.2%	[97]
300–440 °C	40 kW	3020 ppm	99.5%	[97]
300–418 °C	22 kW	634 ppm	98.5%	[97]
300–436 °C	22 kW	595 ppm	98.3%	[97]
600–900 °C	-	0.5–1.1%	90-100%	[98]
1000−1200 °C	-	0.3-0.8%	95%	[99]
400–700 °C	-	3500 ppm	90–100%	[102]

Table 1. Methane removal efficiency of different RTOs, data from [90–92,96].

Prabhu Energy labs has developed a device to counteract the common problems with RTOs. Their device, the Oxiperator, consists of a non-porous section where heat freely transfers from the outlet gas to the inlet gas, and a porous section where oxidation of the methane occurs, as seen in Figure 7. This eliminates the need for the flow to be reversed periodically. The Oxiperator has an operating temperature of approximately 900 °C, meaning heat addition would likely be required for 4-stroke and 2-stroke lean-burn natural gas engines to be effective. The device is scalable, and components can be grouped together to meet the needs of different applications [95].

Energies 2023, 16, 7054 10 of 18

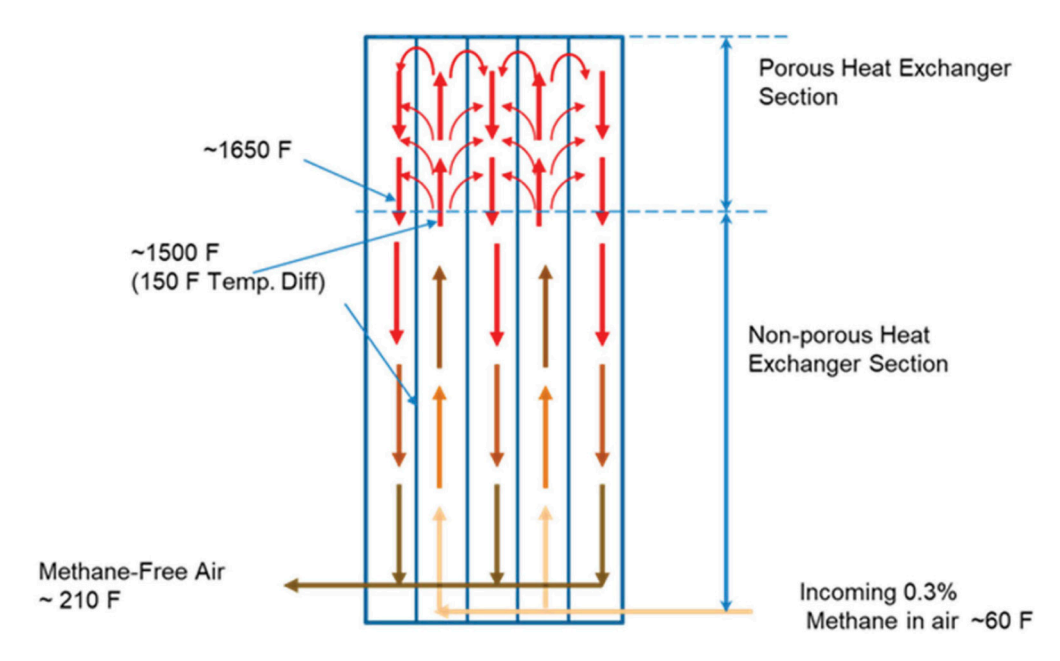


Figure 7. Schematic of Prabhu Energy Labs' Oxiperator [95], (Courtesy Prabhu Energy Labs).

4.3. Exhaust Gas Recirculation

Exhaust gas recirculation (EGR) is a process in which a portion of the exhaust gas is recirculated back into the engine. The methane in the exhaust that is recirculated will be used in the combustion process [15]. Up to 25% of the exhaust is used in an EGR system so 75% of the exhaust goes untreated for methane slip unless another method of methane reduction is used. With EGR rates above 25%, the cylinder pressure and brake efficiency drop off significantly [103]. An EGR cooler is required to cool the exhaust. The EGR cooler can result in water droplets forming, which can increase wear on the turbocharger [15]. An EGR system can result in a 20% reduction in methane emissions [104]. A study performing EGR sweeps on a natural gas engine achieved a 45% reduction in methane emissions using an EGR rate of 14.7% [28]. EGR would need to be paired with another methane emission reduction method such as a catalytic oxidizer or an RTO to achieve a 100% methane reduction. Other benefits of an EGR system are improved combustion stability and a decrease in NO_x emissions [15,104].

5. Hydrogen Blending

Hydrogen is an energy-dense fuel that can be blended with natural gas and used in lean-burn natural gas engines resulting in reduced emissions. When hydrogen is burned, no carbon is produced, and by blending it with natural gas, the amount of carbon released is reduced [5–8]. With minor adjustments, the current natural gas transportation infrastructure can handle hydrogen blends up to 15% [5]. At a hydrogen blend above 20%, the safety risk becomes significantly higher than pure natural gas [5]. With a blend of 20% hydrogen, total hydrocarbon emissions decreased by up to 25% [6,7,9,10]. Emissions of CO₂ and CO were also decreased by 10% [7]. The adiabatic flame temperature of hydrogen is higher than natural gas, which results in an increase in thermal efficiency [9,10]. This also results in an increase in NO_x emissions. The increase in NO_x would need to be addressed by the 3-way catalyst or more EGR for stoichiometric engines or by operating the engine leaner for lean burn engines. Hydrogen blending is not a solution to remove 100% of CH₄ emissions from a lean-burn natural gas engine. Hydrogen blending could be paired with a catalytic or thermal methane oxidation method to achieve complete CH₄ emission removal.

The main obstacle to hydrogen blending is there is no dedicated infrastructure to produce green hydrogen [5]. Green hydrogen is typically hydrogen produced using electrolysis with electricity from green power sources such as wind power, solar power, etc. Blue hydrogen is hydrogen produced using fossil fuels, which results in the production of

Energies **2023**, 16, 7054 11 of 18

hydrogen and CO₂. The production of blue hydrogen includes carbon capture. The current hydrogen production infrastructure generates grey hydrogen. Grey hydrogen is produced the same way as blue hydrogen but does not have carbon capture [5]. By blending grey hydrogen in with natural gas, it is only shifting the carbon emissions earlier in the process. For hydrogen blending to be an effective tool in reducing greenhouse gas emissions, blue or green hydrogen would need to be used.

6. Conclusions

For lean-burn natural gas engines, decreasing valve overlap, trapped methane in crevices, and quenching effects are key ways to decrease the amount of methane slipping into the exhaust. Exhaust treatment methods such as catalytic oxidizers could be effective in reducing the methane of lean-burn natural gas engines.

Palladium-based catalysts and rhodium-based catalysts could achieve nearly 100% methane reduction for 4-stroke engines, operating at temperatures between 395 °C and 530 °C. For the exhaust temperature range of 2-stroke engines, operating between 280 °C and 330 °C, palladium-based catalysts and rhodium-based catalysts would be ineffective. The disadvantage of a palladium catalyst is that it is susceptible to aging and poisoning. Rhodium is resistant to aging and poisoning but is much more expensive than palladium and platinum. The benefit of using a regenerative thermal oxidizer is that there is no risk of aging and poisoning.

Platinum-based catalysts have the advantage of being resistant to aging and being relatively inexpensive. The downside to platinum catalysts is that they are not effective in the temperature ranges of 2-stroke engines. Additionally, nickel-based catalysts would not be an effective catalyst for either 2-stroke or 4-stroke lean-burn natural gas engines.

Platinum-palladium alloys could achieve a nearly 100% reduction in methane emissions at temperatures as low as 325 °C with moderate resistance to aging and poisoning. This is well within the temperature range for 2-stroke and below the temperature range for 4-stroke lean-burn natural gas engines. Pt-Pd catalysts are the best option for catalytic methane reduction. However, they still can be partially affected by poisoning and would not be able to achieve 100% methane reduction at the very bottom portion of the 2-stroke exhaust temperature range.

The benefit of using a regenerative thermal oxidizer is that there is no risk of aging and poisoning. Additionally, RTOs can operate with any exhaust temperature by using heat addition in the oxidation chamber and using the released heat from methane oxidation to preheat the exhaust. RTOs would be most effective in lean-burn natural gas engines. They would not be effective in reducing NO_x emissions that are present at low concentrations in exhaust for lean-burn natural gas engines. The drawback of using many RTOs for natural gas engines is their size, as RTOs are quite large. Smaller thermal oxidizer designs could be effective in natural gas engines.

Methods such as hydrogen blending, at a 20% hydrogen blend, and exhaust gas recirculation can achieve a 20–30% reduction in methane emission for lean-burn natural gas engines. For these methods to achieve a 100% reduction, they must be paired with a catalytic or thermal oxidizer.

7. Future Directions

Catalytic oxidation of methane is a heavily researched topic, but more full-scale testing needs to be conducted, especially on lean-burn natural gas engines. Methane oxidation catalyst formulations that are resistant to degradation and poisoning are needed. Most research regarding thermal oxidizers employed to reduce methane emissions does not focus specifically on using them on lean-burn natural gas engines. Rather, the literature focuses on VAM reduction. Dedicated research using a thermal oxidizer on a lean-burn natural gas engine could prove beneficial. Hydrogen blending and EGR systems are approximately 30% effective at methane emission reduction, and research combining hydrogen blending or

Energies 2023, 16, 7054 12 of 18

an EGR system with a catalytic oxidizer or thermal oxidizer could result in more complete methane emission reductions.

Author Contributions: Conceptualization, A.H. and D.O.; methodology, A.H.; investigation, A.H.; writing—original draft preparation A.H.; writing—review and editing D.O.; visualization A.H. All authors have read and agreed to the published version of the manuscript.

Funding: This research received no external funding.

Data Availability Statement: No new data was created or analyzed in this study. Data sharing is not applicable to this article.

Conflicts of Interest: The authors declare no conflict of interest.

Appendix A

Table A1. Summary of data used to generate Figure 4 and summary of test conditions and performance of several types of oxidation catalysts, data from [33,37–41]. Many of the values of Temperature and Methane Conversion were approximated from graphical data. (NR) denotes no data reported and (N/A) denotes that catalyst did not achieve the corresponding percentage of methane conversions within the test conditions.

Catalyst	Ratio	Density (g/m³)	CH ₄ (ppm)	O ₂ (%)	H ₂ O (%)	SO ₂ (ppm)	Aged	T (°C)	Conversion (%)	Source
Pd	-	10,400	2000	10.5	10	-	No	385	70	[37]
Pd	-	10,400	2000	10.5	10	-	1500 h of use	385	10	[37]
Pd	-	51,800	2000	10.5	10	-	No	385	77	[37]
Pd	-	51,800	2000	10.5	10	-	1500 h of use	385	25	[37]
Pt	-	9600	2000	10.5	10	-	No	385	35	[37]
Pt	-	9600	2000	10.5	10	-	1500 h of use	385	25	[37]
Pt:Pd	1:1	20,800	2000	10.5	10	-	No	385	79	[37]
Pt:Pd	1:1	20,800	2000	10.5	10	-	1500 h of use	385	60	[37]
Pt:Pd	2:3	27,900	2000	10.5	10	-	No	385	80	[37]
Pt:Pd	2:3	27,900	2000	10.5	10	-	1500 h of use	385	55	[37]
Pt:Pd	1:5	12,000	7500	NR	4.89	-	No	325 300 300	100 75 50	[38]
Pt:Pd	3:41	4400	7500	NR	4.89	-	No	525 425 400	100 75 50	[38]
Pt:Pd	3:40	4300	7500	NR	4.89	-	No	350 325 300	100 75 50	[38]
Pt:Pd	10:47	5700	7500	NR	4.89	-	No	375 350 325	100 75 50	[38]
Pd	-	210	7500	NR	4.89	-	No	N/A 550 500	100 75 50	[38]
Pd	-	1400	7500	NR	4.89	-	No	450 400 350	100 75 50	[38]
Pd	-	5297	100,000	20	-	-	No	359 321 282	75 50 25	[39]

Energies 2023, 16, 7054 13 of 18

Table A1. Cont.

Catalyst	Ratio	Density (g/m³)	CH ₄ (ppm)	O ₂ (%)	H ₂ O (%)	SO ₂ (ppm)	Aged	T (°C)	Conversion (%)	Source
Pd	-	5297	100,000	20	-	-	Hydrothermally	426 394 355	75 50 25	[39]
Pd	-	5297	100,000	20	5	-	Hydrothermally	492 452 421	75 50 25	[39]
Pt	-	3355	100,000	20	-	-	No	582 541 477	75 50 25	[39]
Pt	-	3355	100,000	20	-	-	Hydrothermally	634 607 556	75 50 25	[39]
Pt	-	3355	100,000	20	5	-	Hydrothermally	632 604 557	75 50 25	[39]
Pt:Pd	4:10	3355	100,000	20	-	-	No	437 403 360	75 50 25	[39]
Pt:Pd	4:10	3355	100,000	20	-	-	Hydrothermally	471 433 380	75 50 25	[39]
Pt:Pd	4:10	3355	100,000	20	5	-	Hydrothermally	548 497 455	75 50 25	[39]
Pd	-	2260	3000	12	6	-	No	450 400 392	100 75 50	[40]
Pd	-	2260	3000	12	12	-	No	550 450 448	100 75 50	[40]
Pd	-	2260	3000	1.5	12	-	No	N/A	50	[40]
Pt	-	2295	3000	12	6	-	No	N/A	50	[40]
Pt	-	2295	3000	12	12	-	No	N/A	50	[40]
Pt	-	2295	3000	1.5	12	-	No	550 500 500	100 75 50	[40]
Pt:Pd	1:5	2437	3000	12	6	-	No	500 400 393	100 75 50	[40]
Pt:Pd	1:5	2437	3000	12	12	-	No	500 435 427	100 75 50	[40]
Pt:Pd	1:5	2437	3000	1.5	12	-	No	N/A	50	[40]
Rh	-	2 wt%	2500	10	-	-	No	425 350 325	100 75 50	[33]
Rh	-	2 wt%	2500	10	5	-	No	500 400 387	100 75 50	[33]
Rh	-	2 wt%	2500	10	-	20	No	500 462 437	100 75 50	[33]
Rh	-	2 wt%	2500	10	5	20	No	550 487 475	100 75 50	[33]

Energies **2023**, 16, 7054 14 of 18

Table	A1.	Cont

Catalyst	Ratio	Density (g/m³)	CH ₄ (ppm)	O ₂ (%)	H ₂ O (%)	SO ₂ (ppm)	Aged	T (°C)	Conversion (%)	Source
Pd	-	2 wt%	2500	10	-	-	No	462 362 350	100 75 50	[33]
Pd	-	2 wt%	2500	10	5	-	No	475 425 412	100 75 50	[33]
Pd	-	2 wt%	2500	10	-	20	No	550 475 425	100 75 50	[33]
Pd	-	2 wt%	2500	10	5	20	No	N/A 525 512	100 75 50	[33]
Ni:Mg	9:1	6,250,000	10,000	10	10	-	No	550 500 480	100 75 50	[41]
Ni:Mg	9:1	6,250,000	10,000	10	10	-	40 h of use	550 540 504	100 75 50	[41]
Pd	-	1 wt%	10,000	10	10	-	No	450 425 396	100 75 50	[41]
Pd	-	1 wt%	10,000	10	10	-	40 h of use	575 540 507	100 75 50	[41]

References

- 1. Overview of Greenhouse Gases. Available online: https://www.epa.gov/ghgemissions/overview-greenhouse-gases (accessed on 14 August 2023).
- 2. U.S. Environmental Protection Agency. Inventory of U.S. Greenhouse Gas Emissions and Sinks: 1990–2020—Main Text. EPA 430-R-22-003. Available online: https://www.epa.gov/ghgemissions/inventory-us-greenhouse-gas-emissions-and-sinks-1990-2020 (accessed on 14 August 2023).
- 3. Importance of Methane. Available online: https://www.epa.gov/gmi/importance-methane (accessed on 14 August 2023).
- 4. Methane and Climate Change—Global Methane Tracker 2022—Analysis. Available online: https://www.iea.org/reports/global-methane-tracker-2022/methane-and-climate-change (accessed on 14 August 2023).
- 5. Di Lullo, G.; Oni, A.O.; Kumar, A. Blending Blue Hydrogen with Natural Gas for Direct Consumption: Examining the Effect of Hydrogen Concentration on Transportation and Well-to-Combustion Greenhouse Gas Emissions. *Int. J. Hydrogen Energy* **2021**, 46, 19202–19216. [CrossRef]
- Kahraman, N.; Çeper, B.; Akansu, S.O.; Aydin, K. Investigation of Combustion Characteristics and Emissions in a Spark-Ignition engine fuelled with natural gas-hydrogen blends. *Int. J. Hydrogen Energy* 2009, 34, 1026–1034. [CrossRef]
- 7. Park, C.; Kim, C.; Choi, Y.; Won, S.; Moriyoshi, Y. The Influences of Hydrogen on the Performance and Emission Characteristics of a Heavy Duty Natural Gas Engine. *Int. J. Hydrogen Energy* **2011**, *36*, 3739–3745. [CrossRef]
- 8. Katsampes, N.; Montgomery, D.; Arney, G.; Olsen, D.B. Hydrogen-Natural Gas Fuel Blending in a Caterpillar CG137-8 "Rich Burn" Engine with 3-Way Catalyst. In Proceedings of the 13th U.S. National Combustion Meeting Organized by the Central States Section of the Combustion Institute, College Station, TX, USA, 19–22 March 2023.
- 9. Akansu, S.O.; Kahraman, N.; Çeper, B. Experimental Study on a Spark Ignition Engine Fuelled by Methane–Hydrogen Mixtures. *Int. J. Hydrogen Energy* **2007**, 32, 4279–4284. [CrossRef]
- 10. Ma, F.; Wang, Y.; Liu, H.; Li, Y.; Wang, J.; Zhao, S. Experimental Study on Thermal Efficiency and Emission Characteristics of a Lean Burn Hydrogen Enriched Natural Gas Engine. *Int. J. Hydrogen Energy* **2007**, *32*, 5067–5075. [CrossRef]
- 11. Overview of Natural Gas: Background. Available online: http://naturalgas.org/overview/background/ (accessed on 29 September 2023).
- 12. Natural Gas Explained. Available online: https://www.eia.gov/energyexplained/natural-gas/use-of-natural-gas.php#:~:text= Electricity%20generation%20and%20heating%20are,other%20uses%20for%20natural%20gas (accessed on 29 September 2023).
- 13. August 2023 Form EIA-860M. Available online: https://www.eia.gov/electricity/data/eia860m/ (accessed on 29 September 2023).
- 14. About, U.S. Natural Gas Pipelines—Transporting Natural Gas. Available online: https://www.eia.gov/naturalgas/archive/analysis_publications/ngpipeline/index.html (accessed on 29 September 2023).

Energies **2023**, 16, 7054 15 of 18

15. CIMAC WG17 | Methane and Formaldehyde Emissions of Gas Engines. Available online: https://www.cimac.com/publications/publications350/cimac-wg17-methane-and-formaldehyde-emissions-of-gas-engines.html (accessed on 15 August 2023).

- 16. Vaughn, T.L.; Luck, B.; Williams, L.; Marchese, A.J.; Zimmerle, D. Methane Exhaust Measurements at Gathering Compressor Stations in the United States. *Environ. Sci. Technol.* **2021**, *55*, 1190–1196. [CrossRef]
- 17. Learn about the Greenhouse Gas Reporting Program (GHGRP) | Greenhouse Gas Reporting Program (GHGRP) | US EPA. Available online: https://climatechange.chicago.gov/ghgreporting/learn-about-greenhouse-gas-reporting-program-ghgrp#:~:text=The% 20GHGRP%20(codified%20at%2040,sites%20in%20the%20United%20States (accessed on 14 August 2023).
- 18. Subpart W—Petroleum and Natural Gas Systems. Available online: https://www.epa.gov/ghgreporting/subpart-w-petroleum-and-natural-gas-systems (accessed on 14 August 2023).
- 19. Methane Emissions Reduction Program. Available online: https://www.epa.gov/inflation-reduction-act/methane-emissions-reduction-program (accessed on 14 August 2023).
- EPA Proposes to Strengthen Air Quality Standards to Protect the Public from Harmful Effects of Soot. Available online: https://www.epa.gov/newsreleases/epa-proposes-strengthen-air-quality-standards-protect-public-harmful-effects-soot (accessed on 14 August 2023).
- 21. Subpart JJJJ—Standards of Performance for Stationary Spark Ignition Internal Combustion Engines. Available online: https://www.ecfr.gov/current/title-40/chapter-I/subchapter-C/part-60/subpart-JJJJ (accessed on 29 September 2023).
- 22. What Is the Definition of VOC? Available online: https://www.epa.gov/air-emissions-inventories/what-definition-voc (accessed on 29 September 2023).
- 23. Lindblom, J.; Su, W. Methane Slip Prevention in the Combustion Chamber. Bachelor's Thesis, Chalmers University of Technology, Gothenburg, Sweden, 2021.
- 24. Jensen, M.V.; Cordtz, R.F.; Schramm, J. Numerical Analysis of Methane Slip Source Distribution in a Four-Stroke Dual-Fuel Marine Engine. *J. Mar. Sci. Technol.* **2021**, *26*, 606–617. [CrossRef]
- 25. Castillo, A.Q.; Zdanowicz, A.; Windom, B.; Olsen, D. Characterization of Crankcase Ventilation Gas on Stationary Natural Gas Engines. In Proceedings of the 13th U.S. National Combustion Meeting Organized by the Central States Section of the Combustion Institute, College Station, TX, USA, 19–22 March 2023.
- 26. Hiltner, J. *Unburned Hydrocarbon Emissions from Lean Burn Natural Gas Engines*; Sources and Solutions; CIMAC Congress: Helsinki, Finland, 2016.
- 27. Innovative Environmental Solutions, Inc. Optimized Technical Solutions. Availability and Limitations of NOx Emission Control Resources for Natural Gas-Fired Reciprocating Engine Prime Movers Used in the Interstate Natural Gas Transmission Industry; The INGAA Foundation, Inc.: Washington, DC, USA, 2014.
- 28. Hampson, G.J. High Efficiency Natural Gas Engine Combustion Using Controlled Auto-Ignition. In Proceedings of the ASME 2019 Internal Combustion Engine Division Fall Technical Conference; American Society of Mechanical Engineers, Chicago, IL, USA, 20 October 2019; p. V001T03A019.
- Hopoko, M.S. Test Report on Exhaust Emissions from One Solar Mars T-1200 Gas Turbine, Four Cooper Bessemer GMVA-10 Engines, Eight Copper Messemer GMV-10 Engines, and Five Ingersol Rand KVS-12 Engines at the Holbrook Compressor Station; Division of Technical Services and Monitoring Bureau of Air Quality Control: Houston, TX, USA, 1991.
- 30. Olsen, D.B.; Willson, B.D. The Effect of Retrofit Technologies on Formaldehyde Emissions from a Large Bore Natural Gas Engine. *Energy Power Eng.* **2011**, *03*, 574–579. [CrossRef]
- 31. Vieira, G.; Beurlot, K.; Xie, N.; Patterson, M.; Olsen, D. Precombustion Chamber Nozzle Design Effect on Unburned Me-thane Emissions of a Large Bore Two-Stroke Lean- Burn Natural Gas Engine. In Proceedings of the 13th U.S. National Combustion Meeting Organized by the Central States Section of the Combustion Institute, College Station, TX, USA, 19–22 March 2023.
- 32. Forzatti, P.; Lietti, L. Catalyst deactivation. Catal. Today 1999, 52, 165–181. [CrossRef]
- 33. Gélin, P.; Primet, M. Complete Oxidation of Methane at Low Temperature over Noble Metal Based Catalysts: A Review. *Appl. Catal. B Environ.* **2002**, *39*, 1–37. [CrossRef]
- 34. Zhang, Y.; Glarborg, P.; Johansen, K.; Andersson, M.P.; Torp, T.K.; Jensen, A.D.; Christensen, J.M. A Rhodium-Based Methane Oxidation Catalyst with High Tolerance to H₂O and SO₂. *ACS Catal.* **2020**, *10*, 1821–1827. [CrossRef]
- 35. Olsen, D.; Hull, W.; Ginger, P.; Olson, C.; Willson, B. Humidity Control for Power and Emissions; Gas Research Institute: Des Plaines, IL. USA, 2003.
- 36. Defoort, M.; Olsen, D.; Willson, B. Performance Evaluation of Oxidation Catalysts for Natural Gas Reciprocating Engines. In Proceedings of the GMRC Gas Machinery Conference, Nashville, TN, USA, 7–9 October 2002.
- 37. Yamamoto, H.; Uchida, H. Oxidation of Methane over Pt and Pd Supported on Alumina in Lean-Burn Natural-Gas Engine Exhaust. *Catal. Today* **1998**, *45*, 147–151. [CrossRef]
- 38. Worth, D.J.; Stettler, M.E.J.; Dickinson, P.; Hegarty, K.; Boies, A.M. Characterization and Evaluation of Methane Oxidation Catalysts for Dual-Fuel Diesel and Natural Gas Engines. *Emiss. Control. Sci. Technol.* **2016**, 2, 204–214. [CrossRef]
- 39. Abbasi, R.; Huang, G.; Istratescu, G.M.; Wu, L.; Hayes, R.E. Methane Oxidation over Pt, Pt:Pd, and Pd Based Catalysts: Effects of Pre-Treatment. *Can. J. Chem. Eng.* **2015**, *93*, 1474–1482. [CrossRef]
- 40. Gremminger, A.; Pihl, J.; Casapu, M.; Grunwaldt, J.-D.; Toops, T.J.; Deutschmann, O. PGM Based Catalysts for Exhaust-Gas after-Treatment under Typical Diesel, Gasoline and Gas Engine Conditions with Focus on Methane and Formaldehyde Oxidation. *Appl. Catal. B Environ.* 2020, 265, 118571. [CrossRef]

Energies **2023**, 16, 7054 16 of 18

41. Caravaggio, G.; Nossova, L.; Turnbull, M.J. Nickel-Magnesium Mixed Oxide Catalyst for Low Temperature Methane Oxida-tion. *Chem. Eng. J.* **2021**, *405*, 126862. [CrossRef]

- 42. Gélin, P.; Urfels, L.; Primet, M.; Tena, E. Complete Oxidation of Methane at Low Temperature over Pt and Pd Catalysts for the Abatement of Lean-Burn Natural Gas Fuelled Vehicles Emissions: Influence of Water and Sulphur Containing Compounds. *Catal. Today* 2003, 83, 45–57. [CrossRef]
- 43. Nilsson, J.; Carlsson, P.-A.; Martin, N.M.; Adams, E.C.; Agostini, G.; Grönbeck, H.; Skoglundh, M. Methane oxidation over Pd/Al2O3 under rich/lean cycling followed by operando XAFS and modulation excitation spectroscopy. *J. Catal.* **2017**, *356*, 237–245. [CrossRef]
- 44. Farrauto, R.; Hobson, M.; Kennelly, T.; Waterman, E. Catalytic chemistry of supported palladium for combustion of methane. *Appl. Catal. A Gen.* **1992**, *81*, 227–237. [CrossRef]
- 45. Fujimoto, K.-I.; Ribeiro, F.H.; Avalos-Borja, M.; Iglesia, E. Structure and Reactivity of PdOx/ZrO2Catalysts for Methane Oxidation at Low Temperatures. *J. Catal.* 1998, 179, 431–442. [CrossRef]
- 46. Kinnunen, N.M.; Hirvi, J.T.; Venäläinen, T.; Suvanto, M.; Pakkanen, T.A. Procedure to Tailor Activity of Methane Combustion Catalyst: Relation between Pd/PdOx Active Sites and Methane Oxidation Activity. *Appl. Catal. A Gen.* **2011**, *397*, 54–61. [CrossRef]
- 47. Miller, J.B.; Malatpure, M. Pd Catalysts for Total Oxidation of Methane: Support effects. *Appl. Catal. A Gen.* **2015**, 495, 54–62. [CrossRef]
- 48. Narui, K.; Yata, H.; Furuta, K.; Nishida, A.; Kohtoku, Y.; Matsuzaki, T. Effects of Addition of Pt to PdO/Al₂O₃ Catalyst on Catalytic Activity for Methane Combustion and TEM Observations of Supported Particles. *Appl. Catal. A Gen.* **1999**, *179*, 165–173. [CrossRef]
- 49. Strobel, R.; Grunwaldt, J.-D.; Camenzind, A.; Pratsinis, S.E.; Baiker, A. Flame-made Alumina Supported Pd–Pt Nanoparticles: Structural Properties and Catalytic Behavior in Methane Combustion. *Catal. Lett.* **2005**, *104*, 9–16. [CrossRef]
- 50. Lapisardi, G.; Gélin, P.; Kaddouri, A.; Garbowski, E.; Da Costa, S. Pt–Pd bimetallic catalysts for methane emissions abatement. *Top. Catal.* **2007**, 42–43, 461–464. [CrossRef]
- 51. Kinnunen, N.M.; Hirvi, J.T.; Suvanto, M.; Pakkanen, T.A. Methane combustion activity of Pd–PdOx–Pt/Al₂O₃ catalyst: The role of platinum promoter. *J. Mol. Catal. A Chem.* **2012**, *356*, 20–28. [CrossRef]
- 52. Chin, Y.-H.; Buda, C.; Neurock, M.; Iglesia, E. Consequences of Metal–Oxide Interconversion for C–H Bond Activation during CH₄ Reactions on Pd Catalysts. *J. Am. Chem. Soc.* **2013**, *135*, 15425–15442. [CrossRef]
- 53. Lapisardi, G.; Urfels, L.; Gélin, P.; Primet, M.; Kaddouri, A.; Garbowski, E.; Toppi, S.; Tena, E. Superior catalytic behaviour of Pt-doped Pd catalysts in the complete oxidation of methane at low temperature. *Catal. Today* **2006**, *117*, 564–568. [CrossRef]
- 54. Burch, R.; Urbano, F.; Loader, P. Methane combustion over palladium catalysts: The effect of carbon dioxide and water on activity. *Appl. Catal. A Gen.* **1995**, *123*, 173–184. [CrossRef]
- 55. Gholami, R.; Alyani, M.; Smith, K.J. Deactivation of Pd Catalysts by Water during Low Temperature Methane Oxidation Relevant to Natural Gas Vehicle Converters. *Catalysts* **2015**, *5*, 561–594. [CrossRef]
- 56. Schwartz, W.R.; Ciuparu, D.; Pfefferle, L.D. Combustion of Methane over Palladium-Based Catalysts: Catalytic Deactivation and Role of the Support. *J. Phys. Chem. C* **2012**, *116*, 8587–8593. [CrossRef]
- 57. Persson, K.; Pfefferle, L.D.; Schwartz, W.; Ersson, A.; Järås, S.G. Stability of Palladium-Based Catalysts during Catalytic Combustion of Methane: The Influence of Water. *Appl. Catal. B Environ.* **2007**, 74, 242–250. [CrossRef]
- 58. Hurtado, P.; Ordóñez, S.; Sastre, H.; Diez, F.V. Combustion of Methane over Palladium Catalyst in the Presence of Inorganic Compounds: Inhibition and Deactivation Phenomena. *Appl. Catal. B Environ.* **2004**, 47, 85–93. [CrossRef]
- 59. Sadokhina, N.; Smedler, G.; Nylén, U.; Olofsson, M. The Influence of Gas Composition on Pd-Based Catalyst Activity in Methane Oxidation—Inhibition and Promotion by NO. *Appl. Catal. B Environ.* **2017**, 200, 351–360. [CrossRef]
- 60. Lampert, J.K.; Kazi, M.S.; Farrauto, R.J. Palladium Catalyst Performance for Methane Emissions Abatement from Lean Burn Natural Gas Vehicles. *Appl. Catal. B Environ.* **1997**, *14*, 211–223. [CrossRef]
- 61. Monai, M.; Montini, T.; Melchionna, M.; Duchoň, T.; Kúš, P.; Tsud, N.; Prince, K.C.; Matolin, V.; Gorte, R.J.; Fornasiero, P. Phosphorus Poisoning during Wet Oxidation of Methane over Pd@CeO₂/Graphite Model Catalysts. *Appl. Catal. B Environ.* **2016**, 197, 271–279. [CrossRef]
- 62. Kang, S.B.; Hazlett, M.; Balakotaiah, V.; Kalamaras, C.; Epling, W. Effect of Pt:Pd ratio on CO and hydrocarbon oxidation. *Appl. Catal. B Environ.* **2018**, 223, 67–75. [CrossRef]
- 63. Maillet, T.; Solleau, C.; Jacques, B., Jr.; Duprez, D. Oxidation of Carbon Monoxide, Propene, Propane and Methane over a Pd/A1203 Catalyst. Effect of the Chemical State of Pd. *Appl. Catal. B Environ* **1997**, *14*, 85–95. [CrossRef]
- 64. Ribeiro, F.H.; Chow, M.; Dalla Betta, R.A. Kinetics of the Complete Oxidation of Methane over Supported Palladium Catalysts. *J. Catal.* **1994**, 146, 537–544. [CrossRef]
- 65. Sadokhina, N.; Ghasempour, F.; Auvray, X.; Smedler, G.; Nylén, U.; Olofsson, M.; Olsson, L. An Experimental and Kinetic Modelling Study for Methane Oxidation over Pd-based Catalyst: Inhibition by Water. *Catal. Lett.* **2017**, *147*, 2360–2371. [CrossRef]
- 66. Monai, M.; Montini, T.; Melchionna, M.; Duchoň, T.; Kúš, P.; Chen, C.; Tsud, N.; Nasi, L.; Prince, K.C.; Veltruská, K.; et al. The Effect of Sulfur Dioxide on the Activity of hieraRCHical Pd-Based Catalysts in Methane Combustion. *Appl. Catal. B Environ.* **2017**, 202, 72–83. [CrossRef]

Energies **2023**, 16, 7054 17 of 18

67. Sadokhina, N.; Smedler, G.; Nylén, U.; Olofsson, M.; Olsson, L. Deceleration of SO2 poisoning on PtPd/Al2O3 catalyst during complete methane oxidation. *Appl. Catal. B Environ.* **2018**, 236, 384–395. [CrossRef]

- 68. Lou, Y.; Ma, J.; Hu, W.; Dai, Q.; Wang, L.; Zhan, W.; Guo, Y.; Cao, X.; Hu, P.; Lo, G. Low-Temperature Methane Combustion over Pd/H-ZSM-5: Active Pd Sites with Specific Electronic Properties Modulated by Acidic Sites of H-ZSM-5. *ACS Catal.* **2021**, *6*, 8127–8139. [CrossRef]
- 69. Osman, A.I.; Abu-Dahrieh, J.K.; Laffir, F.; Curtin, T.; Thompson, J.M.; Rooney, D.W. A Bimetallic Catalyst on a Dual Component Support for Low Temperature Total Methane Oxidation. *Appl. Catal. B Environ.* **2016**, *187*, 408–418. [CrossRef]
- 70. Petrov, A.W.; Ferri, D.; Tarik, M.; Kröcher, O.; van Bokhoven, J.A. Deactivation Aspects of Methane Oxidation Catalysts Based on Palladium and ZSM-5. *Top. Catal.* **2017**, *60*, 123–130. [CrossRef]
- 71. Petrov, A.W.; Ferri, D.; Kröcher, O.; van Bokhoven, J.A. Design of Stable Palladium-Based Zeolite Catalysts for Complete Methane Oxidation by Postsynthesis Zeolite Modification. *ACS Catal.* **2019**, *9*, 2303–2312. [CrossRef]
- 72. Losch, P.; Huang, W.; Vozniuk, O.; Goodman, E.D.; Schmidt, W.; Cargnello, M. Modular Pd/Zeolite Composites Demonstrating the Key Role of Support Hydrophobic/Hydrophilic Character in Methane Catalytic Combustion. *ACS Catal.* **2019**, *9*, 4742–4753. [CrossRef]
- 73. Venezia, A.; Di Carlo, G.; Liotta, L.; Pantaleo, G.; Kantcheva, M. Effect of Ti(IV) Loading on CH₄ Oxidation Activity and SO₂ tolerance of Pd Catalysts Supported on Silica SBA-15 and HMS. *Appl. Catal. B Environ.* **2011**, 106, 529–539. [CrossRef]
- 74. Jones, J.; Dupont, V.; Brydson, R.; Fullerton, D.; Nasri, N.; Ross, A.; Westwood, A. Sulphur Poisoning and Regeneration of Precious Metal Catalysed Methane Combustion. *Catal. Today* **2003**, *81*, 589–601. [CrossRef]
- 75. Muto, K.-I.; Katada, N.; Niwa, M. Complete Oxidation of Methane on Supported Palladium Catalyst: Support Effect. *Appl. Catal. A Gen.* **1996**, *134*, 203–215. [CrossRef]
- 76. Araya, P.; Guerrero, S.; Robertson, J.; Gracia, F. Methane Combustion over Pd/SiO₂ Catalysts with Different Degrees of hydrophobicity. *Appl. Catal. A Gen.* **2005**, *283*, 225–233. [CrossRef]
- 77. Deng, Y.; Nevell, T.G.; Ewen, R.J.; Honeybourne, C.L. Sulfur Poisoning, Recovery and Related Phenomena over Supported Palladium, Rhodium and Iridium Catalysts for Methane Oxidation. *Appl. Catal. A Gen.* **1993**, *101*, 51–62. [CrossRef]
- 78. Hayes, R.E.; Kolaczkowski, S.T.; Li, P.K.C.; Awdry, S. The Palladium Catalysed Oxidation of Methane: Reaction Kinetics and the e Ect of Di Usion Barriers. *Chem. Eng. Sci.* **2001**, *56*, 4815–4835. [CrossRef]
- Becker, E.; Carlsson, P.-A.; Grönbeck, H.; Skoglundh, M. Methane Oxidation over Alumina Supported Platinum Investigated by Time-Resolved in Situ XANES Spectroscopy. J. Catal. 2007, 252, 11–17. [CrossRef]
- 80. Amin, A.; Abedi, A.; Hayes, R.; Votsmeier, M.; Epling, W. Methane oxidation hysteresis over Pt/Al₂O₃. *Appl. Catal. A Gen.* **2014**, 478, 91–97. [CrossRef]
- 81. Abbasi, R.; Wu, L.; Wanke, S.; Hayes, R. Kinetics of methane combustion over Pt and Pt–Pd catalysts. *Chem. Eng. Res. Des.* **2012**, 90, 1930–1942. [CrossRef]
- 82. Burch, R.; Loader, P.K. Investigation of Pt/Al₂O₃ and Pd/Al₂O₃ catalysts for the combustion of methane at low concentrations. *Appl. Catal. B Environ.* **1994**, *5*, 149–164. [CrossRef]
- 83. Bugosh, G.S.; Easterling, V.G.; Rusakova, I.A.; Harold, M.P. Anomalous Steady-State and Spatio-Temporal Features of Methane Oxidation on Pt/Pd/Al₂O₃ Monolith Spanning Lean and Rich Conditions. *Appl. Catal. B Environ.* **2015**, *165*, 68–78. [CrossRef]
- 84. Gremminger, A.T.; de Carvalho, H.W.P.; Popescu, R.; Grunwaldt, J.-D.; Deutschmann, O. Influence of Gas Composition on Activity and Durability of Bimetallic Pd-Pt/Al₂O₃ Catalysts for Total Oxidation of Methane. *Catal. Today* **2015**, 258, 470–480. [CrossRef]
- 85. Daily Metal Price: Copper Price Chart (USD/Pound) for the Last Month. Available online: https://www.dailymetalprice.com/metalpricecharts.php (accessed on 15 August 2023).
- 86. Liu, F.; Sang, Y.; Ma, H.; Li, Z.; Gao, Z. Nickel Oxide as an Effective Catalyst for Catalytic Combustion of Methane. *J. Nat. Gas Sci. Eng.* **2017**, *41*, 1–6. [CrossRef]
- 87. Ordóñez, S.; Paredes, J.R.; Díez, F.V. Sulphur Poisoning of Transition Metal Oxides Used as Catalysts for Methane Combustion. *Appl. Catal. A Gen.* **2008**, 341, 174–180. [CrossRef]
- 88. González-Cortés, S.L.; Aray, I.; Rodulfo-Baechler, S.M.A.; Lugo, C.A.; Del Castillo, H.L.; Loaiza-Gil, A.; Imbert, F.E.; Figueroa, H.; Pernía, W.; Rodríguez, A.; et al. On the Structure and Surface Properties of NiO/MgO–La₂O₃ Catalyst: Influence of the Support Composition and Preparation Method. *J. Mater. Sci.* 2007, 42, 6532–6540. [CrossRef]
- 89. Pakulska, M.M.; Grgicak, C.M.; Giorgi, J.B. The Effect of Metal and Support Particle Size on NiO/CeO₂ and NiO/ZrO₂ Catalyst Activity in Complete Methane Oxidation. *Appl. Catal. A Gen.* **2007**, 332, 124–129. [CrossRef]
- 90. Ruckenstein, E.; Hu, Y.H. Methane Partial Oxidation over NiO/MgO Solid Solution Catalysts. *Appl. Catal. A Gen.* **1999**, *183*, 85–92. [CrossRef]
- 91. 99/00356 Partial Oxidation of Methane to Syngas over Ni/ MgO, NI/CaO and NI/CeO₂. Fuel Energy Abstr. **1999**, 40, 35. [CrossRef]
- 92. Hu, Y.H.; Ruckenstein, E. The Characterization of a Highly Effective NiO /MgO Solid Solution Catalyst in the CO₂ Reforming of CH4. *Cata. Lett.* **1997**, *43*, 71–77. [CrossRef]
- 93. Saanum, I.; Bysveen, M.; Tunestål, P.; Johansson, B. *Lean Burn versus Stoichiometric Operation with EGR and 3-Way Catalyst of an Engine Fueled with Natural Gas and Hydrogen Enriched Natural Gas*; Lund University: Lund, Sweden, 2007; p. 2007-01-0015.

Energies 2023, 16, 7054 18 of 18

94. Matam, S.K.; Chiarello, G.L.; Lu, Y.; Weidenkaff, A.; Ferri, D. PdO x /Pd at Work in a Model Three-Way Catalyst for Methane Abatement Monitored by Operando XANES. *Top. Catal.* **2013**, *56*, 239–242. [CrossRef]

- 95. Prabhu, E.; Prabhu, M.; Fox, J.E. The Oxiperator for Ventilation Air Methane (VAM). In *Underground Ventilation*; CRC Press: London, UK, 2023; pp. 462–466. ISBN 978-1-00-342924-1.
- 96. Amelio, M.; Morrone, P. Numerical Evaluation of the Energetic Performances of Structured and Random Packed Beds in Regenerative Thermal Oxidizers. *Appl. Therm. Eng.* **2007**, 27, 762–770. [CrossRef]
- 97. Cheng, W.-H.; Chou, M.-S.; Lee, W.-S.; Huang, B.-J. Applications of Low-Temperature Regenerative Thermal Oxidizers to Treat Volatile Organic Compounds. *J. Environ. Eng.* **2002**, *128*, 313–319. [CrossRef]
- 98. Li, Q.; Lin, B.; Yuan, D.; Chen, G. Demonstration and Its Validation for Ventilation Air Methane (VAM) Thermal Oxidation and Energy Recovery Project. *Appl. Therm. Eng.* **2015**, *90*, 75–85. [CrossRef]
- 99. Liu, R.; Liu, Y.; Gao, Z. Methane Emission Control by Thermal Oxidation in a Reverse Flow Reactor. In Proceedings of the 2008 2nd International Conference on Bioinformatics and Biomedical Engineering, Shanghai, China, 18 May 2008; pp. 3952–3955.
- 100. Marín, P.; Díez, F.V.; Ordóñez, S. Reverse Flow Reactors as Sustainable Devices for Performing Exothermic Reactions: Applications and Engineering Aspects. *Chem. Eng. Process.-Process. Intensif.* **2018**, *135*, 175–189. [CrossRef]
- 101. Liu, B.; Hayes, R.; Checkel, M.; Zheng, M.; Mirosh, E. Reversing Flow Catalytic Converter For A Natural Gas/Diesel Dual Fuel Engine. *Chem. Eng. Sci.* **2001**, *56*, 2641–2658. [CrossRef]
- 102. Marín, P.; Hevia, M.A.; Ordóñez, S.; Díez, F.V. Combustion of Methane Lean Mixtures in Reverse Flow Reactors: Comparison between Packed and Structured Catalyst Beds. *Catal. Today* **2005**, *105*, 701–708. [CrossRef]
- 103. Bayliff, S.; Marchese, A.; Windom, B.; Olsen, D. The Effect of EGR on Knock Suppression, Efficiency, and Emissions in a Stoichiometric, Spark Ignited, Natural Gas Engine. In Proceedings of the 2019 WSSCI Fall Technical Meeting Organized by the Western States Section of the Combustion Institute, Albuquerque, NM, USA, 14–15 October 2019.
- 104. Qu, J.; Feng, Y.; Xu, G.; Zhang, M.; Zhu, Y.; Zhou, S. Design and Thermodynamics Analysis of Marine Dual Fuel Low Speed Engine with Methane Reforming Integrated High Pressure Exhaust Gas Recirculation System. *Fuel* **2022**, *319*, 123747. [CrossRef]

Disclaimer/Publisher's Note: The statements, opinions and data contained in all publications are solely those of the individual author(s) and contributor(s) and not of MDPI and/or the editor(s). MDPI and/or the editor(s) disclaim responsibility for any injury to people or property resulting from any ideas, methods, instructions or products referred to in the content.